

Foliar Disease Detection in the Field Using Optical Sensor Fusion

Cedric BRAVO*, Dimitrios MOSHOU*, Roberto OBERTI**, Jon WEST***, Alastair McCartney***, Luigi BODRIA**, Herman RAMON*

* Department of Agro-Engineering and Economics, Katholieke Universiteit Leuven, Kasteelpark Arenberg 30, 3001 Heverlee, Belgium, Email: cedric.bravo@agr.kuleuven.ac.be

** Istituto di Ingegneria Agraria (IIA), University of Milano (UniMI-IIA), via Celoria 2, 20133 Milano, Italia

*** Plant Pathogen Interactions, Rothamsted Research, Harpenden, Hertfordshire AL5 2JQ, Great Britain

ABSTRACT

The objective of this research was to detect and recognize the plant stress caused by disease in the field conditions by combining hyperspectral reflection information between 450 and 900nm and fluorescence imaging. The results can be used to develop a tractor mounted cost-effective optical device for site-specific pesticide application in order to reduce and optimize pesticide use. The work reported here used yellow rust (*Puccinia striiformis*) disease of winter wheat as a model system. In the field hyperspectral reflection images of healthy and infected plants were taken by an imaging spectrograph mounted at spray boom height. Leaf recognition and spectral normalization procedures were used to account for differences in canopy architecture and spectral illumination were used. A model, based on quadratic discrimination, was built, using a selected group of wavebands to differentiate diseased from healthy plants. The model could discriminate diseased from healthy crop with an error of about 10% using measurements from only three wavebands. Multispectral fluorescence images were taken on the same plants using UV-blue excitation. Through comparison of the 550 and 690 nm fluorescence images, the detection of disease was clearly possible. Fraction of pixels in one image, recognized as diseased, was set as final fluorescence disease variable and called the lesion index (LI). The lesion index was added to the pool of normalized selected reflection wavebands. This pool of observations was used in a quadratic discrimination model. The combined model improved disease discrimination compared to either the spectral model or fluorescent model and had a classification error of between 5 and 6 %.

The results suggest that there is a potential for developing detection systems based on multisensor measurements that can be used in precision disease control systems for use in arable crops.

Keywords. spectrograph, imaging fluorescence, hyperspectral imaging, disease detection, sensor fusion, quadratic discrimination, yellow rust

1. INTRODUCTION

The most widely used practice in pest and disease control in arable crops is still to spray pesticides uniformly over fields at different times during the cultivation cycle. However, most disease infestations are not evenly distributed across the field but occur in patches and during the early stages of an epidemic large areas of the field are free of disease. Excessive use of pesticides increases costs and can increase pesticide residue levels on agricultural products. Because pesticides are among the highest components in the production costs of field crops and have been identified as a major contributor to ground water contamination, there is increasing pressure to reduce their use. This can be done by targeting pesticides only on those places in the field where they are needed. Therefore a simple and cost-effective optical device, based on the measurement of canopy reflectance in several wavebands, would allow disease patches to be identified and thus controlled.

Yellow rust (*Puccinia striiformis* f. sp. *tritici*) is an important disease of wheat and was chosen as a model for studying under the OPTIDIS project (EU project, QLK5-1999-01280). The pathogen is wind-dispersed and can rapidly form disease patches, especially in the early stages of an epidemic. Severe epidemics of Yellow rust can reduce yield by up to 7 tons per hectare (Anonymous, 1999). The disease is controlled by a combination of the use of highly resistant cultivars, seed treatment by fungicide, and foliar applications of fungicides (triazole, morpholine and strobilurin).

The pathogen has many asexual reproductive cycles, producing yellow coloured uredospores on leaves during the winter and spring. These spores are wind dispersed in dry weather but require high humidity or wetness films for infection. There is some evidence of rain-splashed dispersal in yellow rust and this plus the tendency of spores to clump together in humid weather so that they are not blown very far can lead to clearly visible yellow patches of disease (Sache, 2000), caused by chlorotic (initial symptoms) and yellow-rusted plants.

Spectral reflectance characteristics of leaves have been shown to be highly correlated with their chemical composition. Carter and Knapp (2001) showed the importance of chlorophyll concentration on the spectral signature of leaves. The spectral reflectance around 700nm was found to be highly correlated with total leaf chlorophyll content. They also investigated the effects of different stress factors including disease. The optical response to stress near 700nm, as well as corresponding changes in reflectance that occur in the green-yellow spectrum, was explained by the general tendency of stress to reduce leaf chlorophyll concentration. The reflection of incident radiation from the leaf interior of stressed plants increases such that stressed plants appear brighter in the visible region of the spectrum than healthy plants (Cibula and Carter, 1992). Riedell and Blackmer (1999) found that leaf reflectance in the 625-635nm and the 680-695nm wavebands together with the NPCI (Normalized total Pigment Chlorophyll a ratio Index) was significantly correlated with the total chlorophyll concentrations in both green bug and Russian wheat aphid-damaged plants. The NPCI is calculated as in equation 1:

$$NPCI = (R_{680} - R_{430}) / (R_{680} + R_{430}) \quad (1)$$

where R_i represents the reflectance at i nm. Polischuk et al. (1997) used spectral reflectance measurements to make an early diagnosis of symptoms of tomato mosaic tobamovirus infection in *Nicotiana debneyi* plants at different growth stages. Reduction in chlorophyll content in the leaves was detected by reflectance measurements less than 10 days after inoculation even although it was three weeks before significant visible differences between healthy and infected plants were noted. Lorenzen and Jensen (1989) obtained similar results for barley leaves infected with cereal powdery mildew. Sasaki et al. (1998) distinguished diseased cucumber leaves from healthy leaves at an early infection stage, based upon the spectral reflectance of the leaves in the 500, 600 and 650nm wavebands. They obtained a classification error of about 10%.

However, most of the above investigations were done in the laboratory and were not related to the field conditions. Boochs et al. (1990) suggested that high-resolution reflectance spectra, especially in the red edge area (reflectance between 680-760nm), would be useful for the identification of small differences in the chemical and morphological status of the plants in the field. It was also suggested that field-based studies could provide as much information as laboratory investigations, if plant health, growing conditions and plant development were strictly controlled. Borel and Gerstl (1994) pointed out that canopy architecture strongly influences illuminated areas for different sun angles, and thus reflectance. This can affect the spectral signature of plants in the field. On the contrary, at a given sun angle, but varying viewing angles, canopy architecture slightly affects spectral signatures and may preserve leaf chemistry signatures.

A small percent of ultraviolet and visible light absorbed by plant's pigments is re-emitted at longer wavelengths as fluorescence in blue, green, red and far-red bands. As this process is in competition with photosynthesis, the efficiency of the photochemistry of the plant, i.e. its physiological status, can be probed by means of chlorophyll fluorescence sensing, allowing to distinguish normal from stressed condition in intact plant material (Cerovic et al., 1999; McMurtrey et al., 2001).

Fluorescence imaging system (FIS) permits to acquire detailed information on local spatial variability of fluorescence pattern across the sample and have been applied in laboratory conditions at microscopic, leaf and plant scale to investigate a wide range of stress symptoms. Daley (1995) studied the effects of tobacco mosaic virus at sub-millimeter scale on tobacco leaves fluorescence, finding high intensity spots in correspondence of the regions where the infection occurred. Peterson and Aylor (1995) found a similar pattern on bean leaves infected by bean rust, stressing that significant chlorophyll fluorescence changes preceded visual symptoms by 3-5 days. Scholes and Rolfe (1996) considered the effects of crown rust on fluorescence of oat leaves, finding again a higher emission by infected regions 3-4 days before the appearance of chlorotic lesions.

More recently multispectral fluorescence imaging systems (MFIS) have been introduced, allowing to acquire images of chlorophyll fluorescence in its different spectral bands, with the aim of investigating the wavelength dependence on the emission according to the stress perturbations. Laboratory researches conducted by Heisel et al. (1996), Lang et al. (1996) and Lichtenthaler et al. (1996) showed that leaves affected by water deficiency and nitrogen deficiency are characterized by a higher blue/red ratio than control leaves; on the opposite, heat stress was found to increase the emission in the red band. Bushmann and Lichtenthaler (1998) reported a dotted pattern of high

intensity spots in blue and green bands with a slight decrease in red and far-red for fluorescence emission of bean leaves affected by mite attack. Kim et al. (2000) found significant differences in red/far-red ratio in leaves treated with herbicide as well as in leaves exposed to elevated ozone concentrations.

Hence, the results reported by researchers show that changes in chlorophyll fluorescence, even if they do not seem to provide a precise and unambiguous information about the stress factor, precede visible indications of stress status of plants, and interesting to investigate further properties in case of disease attacks. Anyway, reflectance disturbance of environmental light is the most severe constraint for field applications of FIS. Johansson et al. (1996) showed the feasibility of remote fluorescence imaging in outdoor conditions by developing a MFIS, based on a pulsed laser synchronized with a gated intensified sensor, able to exclude background illumination and allowing to obtain field images by integrating the acquisition over one hundred laser shots.

The uniqueness of normalized reflectance spectra is discussed by Price (1994). Techniques of spectral unmixing cannot always unambiguously differentiate between different species (or different health status of a given plant species), especially when some spectral signatures are linear combinations of so-called end-points (identification features of other species or plant status). One method to overcome this problem is to make maximum use of variables (e.g. spectral reflectance bands) and less correlated features such as a combination of spectral and fluorescence imaging results. An optimized set-up can also contribute to better measurements (Borel and Gerstl, 1994). The fusion of different measurement approaches, should then provide clearer identification patterns and thus less confusion.

Pre-mapping of diseases and stresses could also be achieved using air-borne systems. Spatial resolutions down to a few meters are possible from satellites and to below 1 m from aircraft (Blakeman et al, 2000). Current commercial satellite sensing is probably not suitable for early disease detection (even if the wavelengths at which data are collected were suitable) because of limitations in spatial resolution. At best, satellite images can be useful by highlighting relatively large areas of disease or other stresses in a crop which can then be checked by the farmer. In addition, revisit time and variability in cloud cover could mean that even this simple information may not be available when required. Aircraft or helicopter mounted systems do not have these constraints and could be used when required. However, data acquisition equipment would likely have to be faster, more sophisticated and more expensive than for terrestrial vehicle-mounted systems.

Several techniques are available to discriminate spectral signals. Moshou et al. (2001) proposed a neural network architecture based on the SOM (Self-Organizing Map) to detect weeds using line spectrography. They successfully compared this architecture with other neural classifiers and classical statistical discrimination based on Minimum Distance Classifier and the Fisher discriminant. Inputs for the neural networks were selected by correlogram analysis. It is possible to detect nitrogen deficiency by using spectral reflection and neural networks as in (Moshou et al., 2003). Also it is possible to detect water deficiency by using fusion of spectral reflection and fluorescence kinetics as in (Moshou et al, 2002).

2. MATERIALS and METHODS

2.1 *Fields, Plants and Material*

2.1.1. Inoculation and growth

Measurements of yellow rust development in winter wheat were taken in 6 plots of 10 x 9 m in size and surrounded by 3 m wide guard rows, located on IACR-Rothamsted's experimental farm. All cultivation were according to local commercial practice (Table 1). Fungicides applied to control other diseases, non-target, when needed.

Table 1. Cultivation detail for the yellow rust experiment (2001 harvest)

Cultivar	Madrigal
Seed rate (N ^o /m ²)	350
Sowing date	6 Oct. 00
Row spacing (cm)	12.5
Previous crop	Lupins
Basal Fungicide against non-target fungi	'Unix' (cyprodinil)

Yellow rust plots were inoculated by putting a 10 cm pot containing 6 infected wheat plants (cv. Madrigal), growing in a peat-based compost, at the center of the plot. The potted plants were inoculated at the second leaf stage (GS 12) by dusting them with uredospores of *P. striiformis*, mixed with 10 parts talcum powder. After inoculation the plants were covered with transparent plastic cloches to maintain a high humidity and were kept at 10°C. The cloches were removed after two days and the plants were transferred to a glasshouse (14-20°C). The inoculation was repeated 7 days after the first one to ensure that all plants would be well colonized. Chlorosis was visible 15 days after the first inoculation (sporulation after about two weeks). The pots were planted in the field on 14 March 2001, approximately three weeks after the first inoculation.

2.1.2. Spectral equipment and data acquisition

The spectral equipment used during the experiments consisted of a digital visual monochromatic camera on which a spectrograph was mounted. The spectrograph measured a line on the canopy and projected a spectrum (between 460-900 nm) for every single area of 0.65mm wide on this line onto the camera, creating a spectral image, with spectral and spatial axes. The length of the measured line was 0.5 m and its width was 4 mm. Light was directed through a 13 mm 1:1.5 C-mount objective into

the spectrograph. An irradiation reference of 50% reflectance (Spectralon SRS 50-010, 38.1 mm diameter, constant 50% reflectance over the 300-2500 nm band) was placed at a constant vertical distance of 70 cm from the objective. It had a flat surface and was positioned horizontally. The equipment was fixed on a buggy, and it was possible to maintain a constant distance between objectives and canopy (Figure 1). The use of the buggy at this stage facilitated the assessment of the feasibility of optical detection of diseases. The use of a buggy is not practical for permanent use. The final disease detection system is planned to be tractor mounted (Fig. 1).

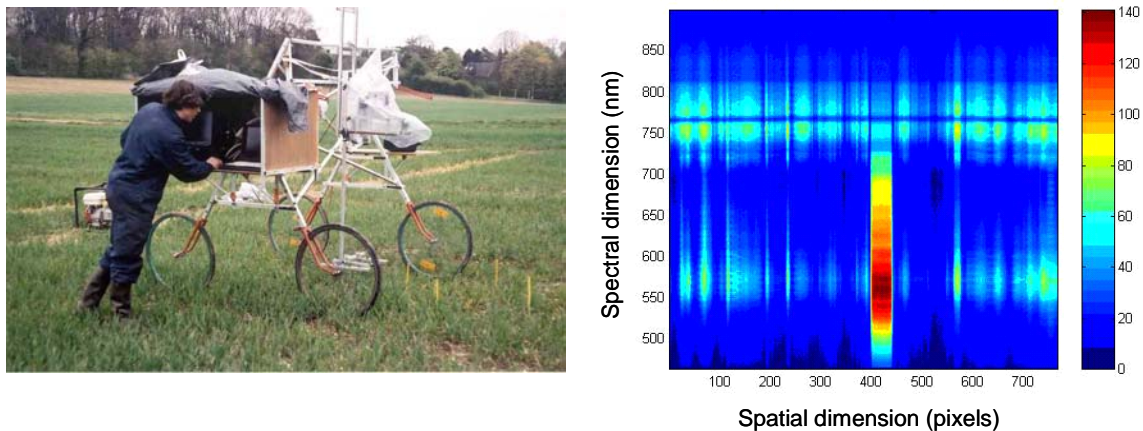


Figure 1. (Left): The buggy on which the spectrograph was mounted. (Right): a spectral image as it was stored.

Measurements were done in plots of winter wheat (cv Madrigal) under ambient conditions. The objectives were positioned at spray boom height (approx. 1m). After data acquisition, the images were loaded as 8-bit matrices with a spectral and a spatial dimension.

2.1.3. Fluorescence imaging: working principle

The multispectral fluorescence imaging system (MFSI) was based on a 10 bits CCD camera with a digital output and a resolution of 1300×1000 pixels approximately, linked with a four bands optical beam splitter. This optical device allowed to split the current field of view of the camera in four identical sub-images, each one independently filtered with pass-band filters (450, 550, 690 and 740nm, all with a FWHM=10nm). Chlorophyll fluorescence was excited by a continuous emitting xenon arc lamp equipped with a IR cut-off filter and a low pass filter with a threshold at 420nm, limiting its emission to the spectral range 350-420nm. The lamp was controlled via a TTL trigger signal by a portable PC, which acquired and stored the images (Fig. 2).

As the intensity of the fluorescence signal is extremely weak, representing a few percent of the actinic light absorbed, compared to the reflected environmental light, background disturbance was reduced by means of an opaque shield which covered the sampled canopy as well as the instrumentation.

For each measurement two consecutive images were acquired. First, a background image was acquired with the xenon lamp off. Immediately after, the second image was acquired when the sample was illuminated by both environmental and additional actinic lights. By subtracting, pixel by pixel, the two images a third image was obtained, representing a “fluorescence map” of the canopy sensed.

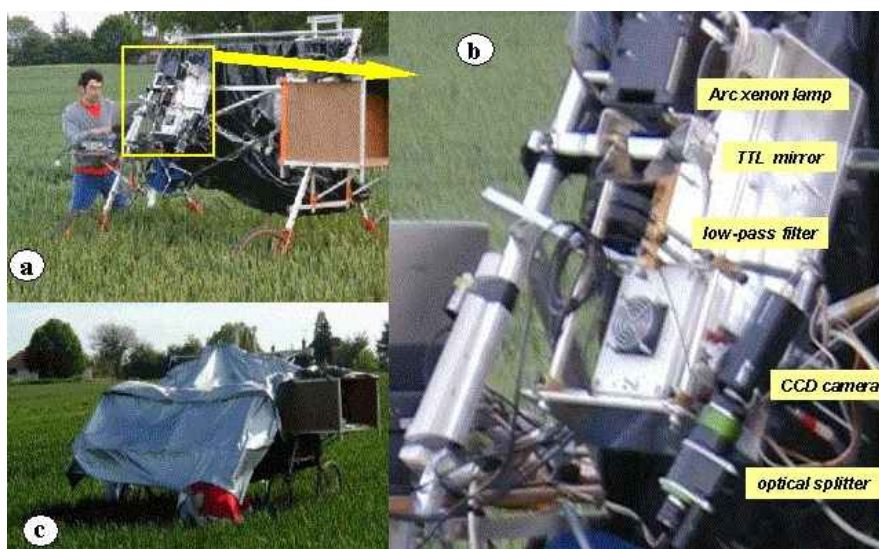


Figure 2. Set-up for field fluorescence imaging: (a) the MSFI mounted on the instrumented buggy; (b) the components of the imaging system; (c) the reflective shield reducing the disturbance of the environmental light on the sensed canopy.

The MFSI (Fig. 2) was mounted on the instrumented buggy and operated from a distance of about 0.8m from the canopy. The area excited to fluorescence by actinic light had a typical diameter of 0.5-0.6m. Fluorescence images at 450, 550, 690 and 740 nm were obtained for canopy areas of about 0.2m diameter, situated in the middle of the illuminated region, resulting in a typical resolution of about 0.3mm/pixel.

Fluorescence images showed typical disease patches. It was observed that disease lesions are characterised by a high emission at 550nm and a low emission at 690nm, where as for a healthy region the fluorescence intensity is quite uniform in the two bands.

The weak fluorescence signal and environmental noise made the precise fluorescence measurement difficult. To compensate for these variations only well illuminated vegetation pixels, determined by

an adaptive threshold were included in the analysis. The retained regions were then spatially filtered in order to eliminate the noise spots and to fill possible “holes” in closed areas, obtaining the vegetation region to be inspected.

Based on this, just the images in the two fluorescence bands 550nm and 690nm were used and a disease index for each pixel was defined as the relative intensity in the two bands, f_G (Equation 2).

$$f_G = \frac{I_{550nm}}{I_{550nm} + I_{690nm}} \quad (2)$$

A pixel was assumed to be “diseased” when f_G exceeded 0.65. A lesion index (LI), defined as the fraction of the analyzed pixels that were “diseased” ($f_G > 0.65$), and representing the suspected diseased area, was calculated for each image. Only well illuminated vegetation pixels, determined by an adaptive threshold were included in the analysis.

2.2 Spectral Data Normalization

2.2.1. Leaf selection

In order to analyse the entire spectral signature of the canopy, it was important to select the plant which was only in the specific spectra. The normal differential vegetation index (NDVI), is a good parameter for leaf detection (Rouse et al., 1974) and is defined through Equation 3:

$$NDVI = \frac{NIR - R}{NIR + R} \quad (3)$$

where NIR represents the reflectance in the near infrared band (740-760nm) and R the reflectance in the red band (640-620nm). The spreading of the NDVI over a plant (or an entire plot) characterizes the state of the plant (age, leaf area index, health in some extend). The method proposed here considered the entire canopy, since disease can occur anywhere on the plant. Therefore all leaf surfaces had to be taken into account, without interference from the soil or other sources. NDVI's were examined and lower and upper values that allowed the maximum number of leaves to be identified were chosen. After reflectance normalization (division of the canopy spectral reflection through the illumination spectrum), the spectra were also normalized for differences in canopy architecture by adjusting for illumination intensity. The illumination was indirectly measured by a spectralon 50% reflectance included in the spectral image (Fig. 1). The spectralon had a 50% constant reflectance over the 200-2000nm waveband. Suppose that the spectral image can be written as matrix A, then the normalized matrix B can be defined as below:

$$B(s, \lambda) = 50\% * \frac{A(s, \lambda)}{\sum_{460nm}^{900nm} A(s, \lambda_i)} * \frac{\sum_{460nm}^{900nm} A(ref, \lambda_i)}{A(ref, \lambda)} \quad (4)$$

where s is the observation number along the spatial axis, λ is the waveband and ref is the position of the reference (spectralon) along the spatial axis (in pixel numbers).

By opting to identify a maximum number of leaves, the canopy spectra were highly variable. Single spectra were therefore subjected to high levels of noise resulting in low discrimination, even after intensity normalization. Since infected leaves are mostly surrounded by other diseased leaves (see the patches in which the disease develops), it was decided to average the spectra in the spatial dimension with a 20cm wide moving window, in order to reduce the variability. Consequently the variance of one waveband reflectance decreased, but its mean stayed the same allowing discrimination.

2.2.2. Illumination independence

The effect of different illumination levels on normalized spectral signatures was investigated by correlating the normalized spectral output at each wavelength with the illumination at the same wavelength (Fig. 3)

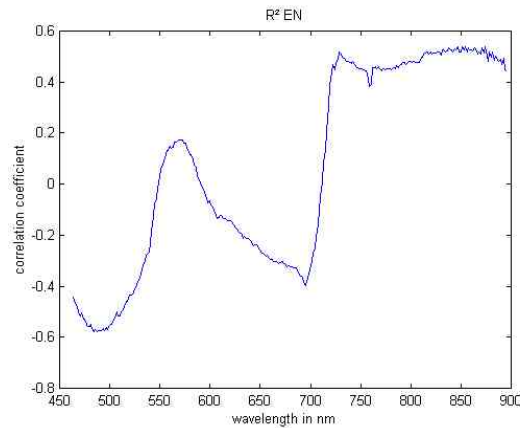


Figure 3. The distribution of correlation coefficients with wavelengths for the correlation of normalized spectra with illumination at the same wavelength measured on May 29th, 2002.

Subsequent linear regressions of the relationships between illumination at all wavebands and reflectance at the same wavebands were therefore applied in last normalization step (Equation 5).

$$B(s, \lambda) = a * A(ref, \lambda) + b \quad (5)$$

where $B(s, \lambda)$ is the average reflectance of one image in a given waveband, $A(s, \lambda)$ the illumination in the same waveband, a and b are waveband related regression coefficients. The final normalized spectral output at a certain waveband, $NewSpec(s, \lambda)$, was defined in Equation 6:

$$NewSpec(s, \lambda) = \frac{B(s, \lambda) - b}{a * A(ref, \lambda) + const} \quad (6)$$

The constant ($const$) was required to avoid numerical problems (division with small numbers) that could lead to unreliable results (here the constant was chosen equal to 50).

2.3 Data handling

2.3.1. Waveband selection

In order to find best discriminating wavebands between diseased and healthy spectra, wavebands were found through a stepwise variable selection. The procedure was based on the following: a waveband was only selected when its addition to the existing set of selected wavebands significantly increased the discriminating power of the new set of wavebands as determined by an F-test; and before a new waveband was chosen, the already chosen wavebands were investigated for the significance of their presence in the selected set. The ultimate selection was then used to build the discrimination model.

2.3.2. Quadratic Discriminant Analysis (QDA)

Once the most discriminating set of wavebands was selected, a simple discrimination rule was defined. This criterion, called the quadratic classification rule, was based on the Mahalanobis distance of a single observation (average of normalized spectra over a fixed window) to the class means (healthy or diseased). An observation was then classified according to the smallest Mahalanobis distance to a class mean. The criterion was trained on 75% of the data. The discrimination models were thereafter validated by a test dataset using the other 25% of all data.

3. RESULTS and DISCUSSION

3.1. Spectrographic Disease Detection

Spectrographic results for disease detection using three 20nm wide wavebands (680, 725 and 750 nm) are shown in Table 2.

Table 2. Different classification results for spectrographic measurements obtained using QDA.

Observations expressed in % classified into each category			
Status	Classified Healthy	Classified Diseased	Total
Healthy	90.23 %	9.77 %	100 %
Diseased	12.75 %	87.25 %	100 %

3.2. *Imaging Fluorescence Disease Detection*

For all measurements LI values were determined and saved in appropriate format to be fused with spectral measurements for the same measured field areas. Typical values obtained were: LI=0 - 0.07 for a healthy canopy; LI=0.05 - 0.20 for a slightly infected canopy; LI=0.35 - 0.60 for a disease focus. The values of LI for healthy canopies showed small overlap with the values obtained from slightly infected plants. This means that a discrimination algorithm using LI as a feature can not separate completely healthy from slightly infected plants. QDA results from the LI are shown in Table 3.

Table 3. Disease classification results for fluorescence imaging measurements obtained using QDA.

Observations expressed in % classified into each category			
Status	Classified Healthy	Classified Diseased	Total
Healthy	71.43 %	28.57 %	100 %
Diseased	4.35 %	95.65 %	100 %

3.3. *Sensor Fusion Results*

In order to design a practical optical sensor that can discriminate between healthy and diseased canopies it is important to reduce the number of selected wavebands to a minimum which can still maintain discrimination. The best results were obtained using the largest possible spatial window width on the spectrographic data. Quadratic Discriminant Analysis (QDA) was used for disease detection based on the features identified from the F-test waveband selection. Three 20 nm wide wavebands (680, 725 and 750 nm) that gave the best discrimination were selected. A total of four fusion features were used: 3 spectral reflectance values and the fluorescence parameter, LI. The two 20 nm wide wavebands (750 and 680 nm) were also used for leaf detection by NDVI. Disease discrimination results derived from a fusion of these measurements are presented in Table 4.

Table 4. Disease classification results derived from the fusion of sensor measurements obtained from the test dataset using QDA.

Status	Observations expressed in % classified into each category		
	Classified Healthy	Classified Diseased	Total
Healthy	97.78 %	2.22 %	100 %
Diseased	8.86 %	91.14 %	100 %

4. CONCLUSIONS

Although previous laboratory studies have shown that optical techniques have the potential to discriminate between diseased and healthy plants, the experiments reported here demonstrate the feasibility of using such methods for disease detection under field conditions. Two separate approaches were used: first one was based on spectral reflectance measurements and second one was based on fluorescence induction. The spectral reflection method, based on only three wavebands, was developed that could discriminate the disease with an error of about 10%. The method based on fluorescence was less accurate (discrimination error of about 25%), because it used only two fluorescence wavebands. However, combining the measurements from the two approaches allowed disease discrimination with accuracy between 94 and 95%.

The results of these experiments clearly demonstrate that techniques based on the fusion of measurements from different optical sensors have great potential for developing tractor-based systems for disease detection in the field. However, further research is necessary to develop and test practical systems that could be incorporated into management programs for controlling foliar diseases of arable crops.

5. ACKNOWLEDGEMENTS

This research has been performed as part of the OPTIDIS project. The OPTIDIS project is funded by the EC under the Quality of Life Programme – Framework V.

6. REFERENCES

Anonymous. 1999. Controlling yellow rust on winter wheat. Topic Sheet 21, Spring, Home-Grown Cereals Authority

C. Bravo, D. Moshou, R. Oberti, J. West, A. McCartney, L. Bodria, and H. Ramon. "Foliar Disease Detection in the Field Using Optical Sensor Fusion". *Agricultural Engineering International: the CIGR Journal of Scientific Research and Development*. Manuscript FP 04 008. Vol. VI. December, 2004.

- Blakeman, R.H., R. J. Bryson and P. Dampney. 2000. Assessing crop condition in real time using high resolution satellite imagery. In *Aspects of Applied Biology 60, Remote sensing in agriculture*, eds. R. J. Bryson, W. Howard, A. E. Riding, L. P. Simmonds and M. D. Steven, 163-171. Wellesbourne, UK: The Association of Applied Biologists.
- Boochs, F., G. Kupfer, L. Dockter and W. Kühbauch. 1990. Shape of the red edge as vitality indicator for plants. *International Journal of Remote Sensing* 11(10): 1741-1753.
- Borel, C. C. and S. A. W. Gerstl. 1994. Are leaf chemistry signatures preserved at the canopy level? In *Proc. IGARSS' 94 International Geoscience and Remote Sensing Symposium*, eds. IEEE, 996-998. Pasadena, Ca., 8-12 August.
- Bushmann C. and H. Lichtenthaler. 1998. Principles and characteristics of multicolour fluorescence imaging system. *Journal of plant physiology* 152: 297-314.
- Carter, G. A. and A. K. Knapp. 2001. Leaf optical properties in higher plants: linking spectral characteristics to stress and chlorophyll concentration. *American Journal of Botany* 88(4): 677-684.
- Cerovic Z., G. Samson, F. Morales, N. Tremblay and I. Moya. 1999. Ultraviolet induced fluorescence for plant monitoring: present state and prospects. *Agronomie* 19: 543-578.
- Cibula, W. G. and G. A. Carter. 1992. Identification of a far-red reflectance response to ectomycorrhizae in slash pine. *International Journal of Remote Sensing* 13(5): 925-932.
- Daley P. 1995. Chlorophyll fluorescence analysis and imaging in plant stress and disease. *Canadian journal of plant pathology* 17(2): 167-173.
- Heisel F., M. Sowinska, J. Miehe and H. Lichtenthaler. 1996. Detection of nutrient deficiencies of maize by laser induced fluorescence sensing. *Journal of plant physiology* 148: 622-631.
- Johansson J., M. Andersson, H. Edner, J. Mattson and S. Svanberg. 1996. Remote fluorescence measurements of vegetation spectrally resolved by multicolour fluorescence imaging. *Journal of plant physiology* 148: 632-637.
- Kim M., J. McMurtrey, C. Mulchi, C. Daughtry, E. Chappelle and Y. Chen. 2000. Steady-state multispectral fluorescence imaging system for plant leaves. *Applied Optics* 40(1): 157-166.
- Lang M., H. Lichtenthaler, M. Sowinska, F. Heisel and J. Miehe. 1996. Fluorescence imaging of water and temperature stress in plant leaves. *Journal of plant physiology* 148: 613-621.
- Lichtenthaler H., M. Lang, M. Sowinska, F. Heisel and J. Miehe. 1996. Detection of vegetation stress via a new high resolution fluorescence imaging system. *Journal of plant physiology* 148: 599-612.
- Lorenzen, B. and A. Jensen. 1989. Changes in spectral properties induced in Barley by cereal Powdery Mildew. *Remote Sensing of Environment* 27(2): 201-209.

- McMurtrey J.E., L.A. Corp, M.S. Kim, E.M. Chappelle, C.S.T. Daughtry and J. DiBenedetto. 2001. Fluorescence techniques in agricultural applications. In *Optics in agriculture 1999-2000*, eds. J. De Shazer and G. Meyer, 80:37-64. Bellingham (USA): SPIE.
- Moshou, D., E. Vrindts, B. De Ketelaere, J. De Baerdemaeker and H. Ramon. 2001. A neural network based plant classifier. *Computers and Electronics in Agriculture* 31(1): 5-16.
- Moshou D., C. Bravo and H. Ramon. 2002. Neural Network based Multisensor Fusion applied in water stress and disease recognition. In *Proc. AgEng2002 International Conference on Agricultural Engineering*; Budapest, Hungary, 30 June-4 July.
- Moshou D., C. Bravo, S. Wahlen, J. West, A. McCartney, J. De Baerdemaeker and H. Ramon. 2003. Simultaneous identification of plant stresses and diseases in arable crops based on a proximal sensing system and Self-Organizing Neural Networks. In *Precision Agriculture*, eds. J. Stafford and A. Werner, 425-432. Wageningen, The Netherlands: Wageningen Academic Publishers.
- Peterson R. and D. Aylor. 1995. Chlorophyll fluorescence induction in leaves of *Phaseolus Vulgaris* infected with bean rust. *Plant physiology* 108: 163-171.
- Polischuk, V. P., T.M. Shadchina, T.I. Kompanetz, I.G. Budzanivskaya and A.A. Sozinov. 1997. Changes in reflectance spectrum characteristic of *Nicotiana debneyi* plant under the influence of viral infection. *Archives of Phytopathology and Plant Protection* 31(1): 115-119.
- Price, J. C. 1994. How unique are spectral signatures? *Remote Sensing of Environment* 49(3): 181-186
- Riedell, W. E. and T. M. Blackmer. 1999. Leaf reflectance spectra of cereal aphid-damaged wheat. *Crop Science* 39(6): 1835-1840.
- Rouse, J. W. Jr., R.H. Haas, D.W. Deering, J.A. Schell and J.C. Harlan. 1974. Monitoring the Vernal Advancement and Retrogradation (Green Wave Effect) of Natural Vegetation. *NASA/GSFC Type III Final Report, Greenbelt, MD.*, 371.
- Sache, I. 2000. Short-distance dispersal of wheat rust spores by wind and rain. *Agronomie* 20: 757-767.
- Sasaki, Y., T. Okamoto, K. Imou and T. Torii. 1998. Automatic diagnosis of plant disease-Spectral reflectance of healthy and diseased leaves. In *Proc. AgEng98 International Conference on Agricultural Engineering*, Oslo, Norway, 23-27 August.
- Scholes J. and S. Rolfe. 1996. Photosynthesis in localised regions of oat leaves infected with crown rust quantitative imaging of chlorophyll fluorescence. *Planta*. 199: 573-582.